Hindawi Publishing Corporation
International Journal of Corrosion
Volume 2012, Article ID 894875, 5 pages
doi:10.1155/2012/894875

Research Article

The Effect of Applied Stress on Environment-Induced Cracking of Aluminum Alloy 5052-H3 in 0.5 M NaCl Solution

Osama M. Alyousif[1] and Rokuro Nishimura[2]

[1] *Department of Mechanical Engineering, College of Engineering & Petroleum, Kuwait University, P.O. Box 5969, Safat 13060, Kuwait*
[2] *Department of Applied Materials Science, College of Engineering, Osaka Prefecture University, 1-1, Gakuen-cho, Sakai, Osaka 599-8531, Japan*

Correspondence should be addressed to Osama M. Alyousif, osama.alyousif@ku.edu.kw

Received 31 March 2012; Accepted 17 May 2012

Academic Editor: Nobuyoshi Hara

The environment-induced cracking (EIC) of aluminum alloy 5052-H3 was investigated as a function of applied stress and orientation (Longitudinal rolling direction—Transverse: LT and Transverse—Longitudinal rolling direction: TL) in 0.5 M sodium chloride solution (NaCl) using a constant load method. The applied stress dependence of the three parameters (*time to failure; t_f, steady-state elongation rate, l_{ss}, and transition time at which a linear increase in elongation starts to deviate, t_{ss}*) obtained from the corrosion elongation curve showed that these relationships were divided into three regions, the stress-dominated region, the EIC- dominated region, and the corrosion-dominated region. Aluminum alloy 5052-H3 with both orientations showed the same EIC behavior. The value of t_{ss}/t_f in the EIC-dominated region was almost constant with 0.57 ± 0.02 independent of applied stress and orientation. The fracture mode was transgranular for 5052-H3 with both orientations in the EIC-dominated region. The relationships between $\log I_{ss}$ and $\log t_f$ for 5052-H3 in the EIC-dominated region became a good straight line with a slope of -2 independent of orientation.

1. Introduction

The environment-induced cracking (EIC) behavior of metallic alloys in chloride and other corrosive solutions has been extensively investigated using various EIC methods [1–7], where EIC is composed of stress corrosion cracking (SCC) subjected to anodic reactions such as film formation and dissolution and hydrogen embrittlement (HE) to cathodic reactions such as hydrogen evolution. A number of theories have been developed for cracking mechanisms of aluminum alloys in chloride environments [5–9]. Suresh et al. have concluded that EIC behavior in high-strength 7075 aluminum alloy under fatigue loading is mostly governed by three mechanisms, namely, the embrittling effect by the hydrogen products of the electrochemical reactions at the crack tip, the role of microstructure and slip mode and crack closure arising from environmental and microstructural elements [8, 9].

It has been reported that the behavior of the metallic alloy can be characterized using a constant load method [10]. The method can produce a corrosion elongation curve which can be used to obtain three parameters, namely, time to failure (t_f), steady-state elongation rate (l_{ss}), and transition time at which a linear increase in elongation starts to deviate (t_{ss}). These parameters were confirmed to be used in analyzing the failure behavior and to predict time to failure (t_f) [11, 12].

The objectives of this research work are (1) to investigate the effect of applied stress on the susceptibility of aluminum alloys to EIC, (2) to evaluate the role of orientation in alloys, and (3) to elucidate a qualitative cracking mechanism for aluminum alloys in the chloride solution.

2. Experimental

The specimens used were made out of commercial 5052-H3 aluminum alloy. The geometry for EIC experiments was as follows: the gauge length 25.6 mm, its width 5 mm, and the thickness 1 mm. The specimen geometry is shown in Figure 1. The sample orientation used for the experiments

Table 1: Chemical compositions (wt%) and mechanical properties of A5052-H3 aluminum alloy used.

	Cu	Si	Fe	Mn	Mg	Zn	Cr	Ti	Al	σ_{Yield} (MPa)	σ_{Tensile} (MPa)
A5052-H34	0.01	0.08	0.26	<0.001	2.59	<0.001	0.17	—	Bal.	180	251

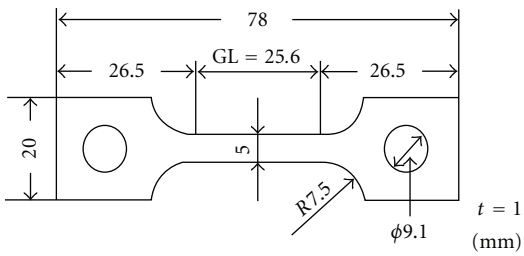

Figure 1: Geometry of the specimens (dimensions in mm).

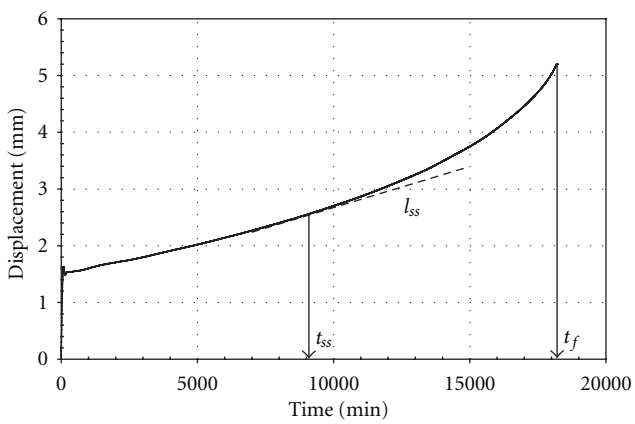

Figure 2: The corrosion elongation curves for A5052-H3-LT at T = 353 K and σ = 240 MPa in 0.5 M sodium chloride solution.

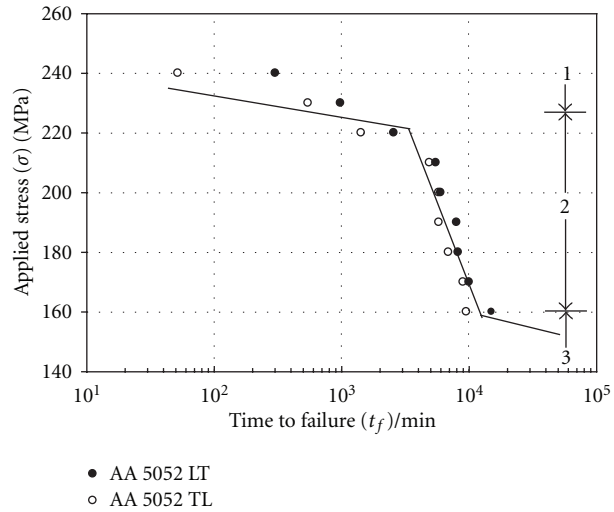

Figure 3: The logarithm of time to failure (t_f) versus applied stress (σ) for A5052-H3 in a 0.5 M sodium chloride solution.

was TL (Transverse—Longitudinal rolling direction) and LT (Longitudinal rolling direction—Transverse) where, in the TL orientation, the former T is the loading direction and the later L is the direction of crack growth whereas, in the LT specimens, the loading direction is in the longitudinal (L) direction and the crack growth direction is the T direction.

The chemical composition (wt%) for aluminum alloy 5052-H3 used was shown in Table 1. Prior to the experiments, the specimens were polished to 600 grit emery paper, degreased with acetone in an ultrasonic cleaner, and washed with distilled water. After the pretreatment, the specimens were immediately set into an SCC cell. The SCC tests were conducted in 0.5 M sodium chloride solutions at a test temperature of 353 K. The applied stress range for aluminum alloy 5052-H3 was from 140 MPa to 240 MPa. All experiments were carried out under an open-circuit condition.

A lever-type constant load apparatus (lever ratio 1 : 10) to which three specimens can be separately and simultaneously attached was used with a cooling system on the top to avoid evaporation of the solution during the experiments. The specimens were insulated from rod and grip by surface-oxidized zirconium tube. A change in elongation of the specimens under the constant load condition was measured by an inductive linear transducer with an accuracy of ±0.01 mm.

3. Results

3.1. Corrosion Elongation Curve. Figure 2 shows an example of the corrosion elongation curve for 5052-H3 with the LT orientation at a test temperature of 353 K and an applied stress of 240 MPa in 0.5 M sodium chloride solution. From this curve the three parameters were obtained: time to failure (t_f), steady-state elongation rate (l_{ss}) for the straight part of the corrosion elongation curve, and transition time (t_{ss}), which is the time when the elongation curve begins to deviate from the linear increase and is indicated as t_{ss}/t_f in the paper.

3.2. Applied Stress Dependence of Three Parameters (t_f, l_{ss}, and t_{ss}/t_f). Figure 3 depicts the logarithm of time to failure (t_f) versus applied stress (σ) for 5052-H3 with the TL and LT orientations in a 0.5 M sodium chloride solution at a test temperature of 353 K. The relationships fell into three regions shown by Arabic numerals 1–3 in the figures, whereas the applied stress dependence of t_f was identical independent of the orientation. Figure 4 shows the relationship between the logarithm (l_{ss}) and applied stress (σ). The relationships were also divided into three regions with the same applied stress ranges as those in Figure 3. The value of l_{ss} in region 3 became significantly small compared to those in region 2, although this is not clear in Figure 3. Figure 5 shows the relationship between t_{ss}/t_f and σ. The value of t_{ss}/t_f was divided into three regions with the same

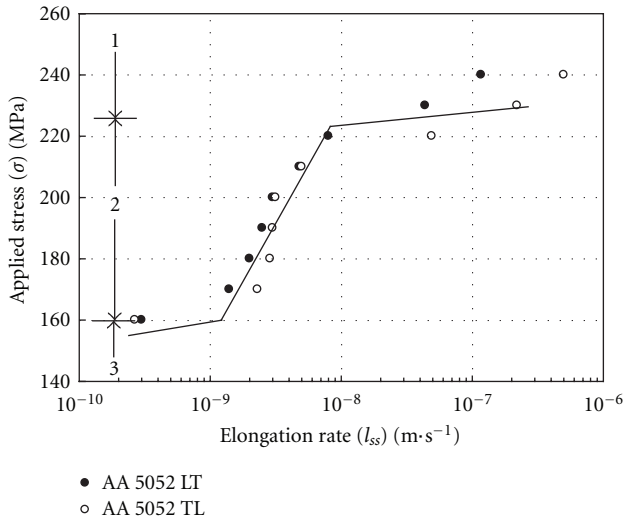

Figure 4: The logarithm of steady-state elongation rate (l_{ss}) versus applied stress (σ) for A5052-H3 in a 0.5 M sodium chloride solution.

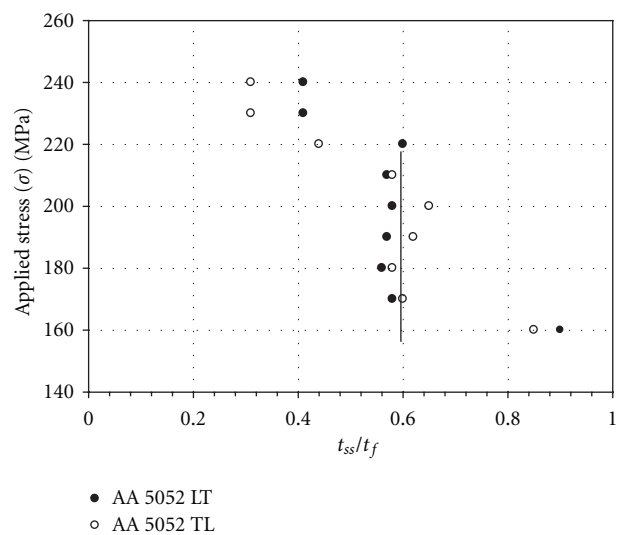

Figure 5: The logarithm of (t_{ss}/t_f) versus applied stress (σ) for A5052-H3 in a 0.5 M sodium chloride solution.

applied stress ranges as those in Figures 3 and 4. The value of t_{ss}/t_f in region 2 kept constant with 0.57 ± 0.02 independent of applied stress and orientation. However, that of t_{ss}/t_f in region 3 was 0.8 to 0.9 irrespective of orientation, while in region 1 it became smaller with a value of 0.3 to 0.4.

Thus, the applied stress dependences of three parameters were divided into three regions (regions 1 to 3). In region 1 t_f decreased rapidly with increasing applied stress with the rapid increase in l_{ss}. In region 2 $\log t_f$ increased and $\log l_{ss}$ decreased linearly with decreasing applied stress and in region 3 $\log t_f$ was not clear for deviation from the liner relationship in region 2, but $\log l_{ss}$ showed clearly deviation. This behavior was almost the same as those for the solution annealed and sensitized austenitic stainless steels [13–16] and pure titanium [17]. Therefore, it was decided that region 1 was the stress-dominated, region 2 the EIC-dominated region, and region 3 the corrosion-dominated region, respectively.

3.3. Fracture Appearance. The fracture appearances of 5052-H3 with both orientations were investigated by using the scanning electron microscopy. Figure 6 shows the fracture appearance of 5052-H3 with the LT orientation in the EIC-dominated region (region 2). It was found that the fracture mode was predominantly transgranular (TG) with a dimple pattern, which was observed over the whole applied stresses in the EIC-dominated region.

4. Discussion

4.1. A Parameter for Predicting Time to Failure. Figure 7 shows the relationship between $\log t_f$ and $\log l_{ss}$ for 5052-H3 with both orientations, which was obtained by using those in Figures 3 and 4. The $\log t_f$ versus $\log l_{ss}$ curve in the EIC-dominated region for 5052-H3 became a straight line with a slope of $m = -2$ independent of orientation. Thus, we got the empirical equation as expressed in the following:

$$\log l_{ss} = -2 \log t_f + C_1, \tag{1}$$

where C_1 is a constant.

From (1), it was found that l_{ss} becomes a useful parameter for predicting t_f independent of applied stress as well as for austenitic stainless steels in hydrochloric acid and sulphuric acid solutions [8], because l_{ss} can be obtained at a time within 10–20% of t_f from the corrosion elongation curve.

4.2. A Qualitative Proposal of EIC Mechanism. In general, the fracture mode of aluminum alloys is recognized to be intergranular [18]. In 5xxx series alloys, a precipitate of Mg_2Al_3 is considered to exist along a grain boundary and to become anodic compared to grain itself [18], which may suggest that the EIC of 5052-H3 would be an intergranular stress corrosion cracking (IG-SCC). However, the present fracture mode was transgranular. This means that the precipitate would not affect the EIC behavior under the present experimental condition.

As for the EIC of the solution annealed and sensitized austenitic stainless steels in boiling saturated magnesium chloride solutions [13–16], when the EIC was TGSCC, the value of t_{ss}/t_f was 0.57 ± 0.02 and the slope of the linear relationship between $\log t_f$ and $\log l_{ss}$ was −2. On the other hand, in the case of HE, the value of t_{ss}/t_f was 0.8 ± 0.02 and the slope of the linear relationship was −1, which were similar to those for HE of pure titanium [17]. Therefore, the present results obtained suggest that the EIC of 5052-H3 is TGSCC and would be explained by adopting the TGSCC mechanism of the austenitic stainless steels. The TGSCC was based on a cyclic film rupture-formation event. A crack is initiated at slip steps and a film formed at the crack tip inhibits dislocation movement, which is enhanced by metal dissolution. As a result, a dislocation pileup takes place and

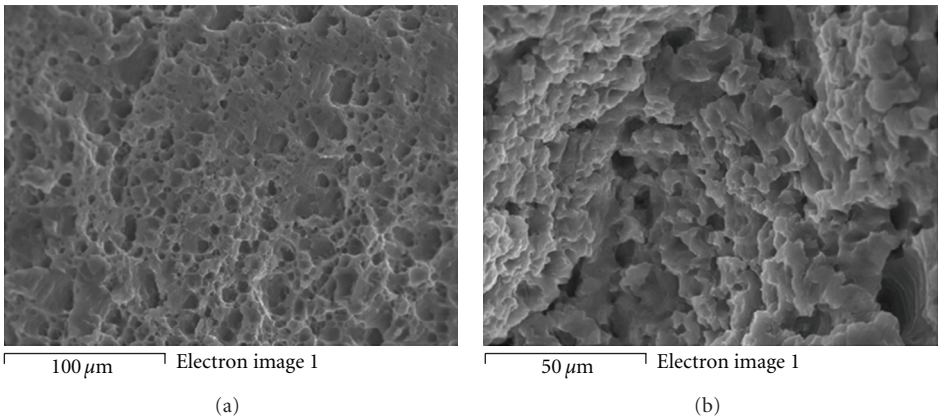

Figure 6: Fracture appearances for A5052-H3 at T = 353 K and σ = 230 MPa; X550, LT orientation (a), TL orientation (b) in 0.5 M sodium chloride solution.

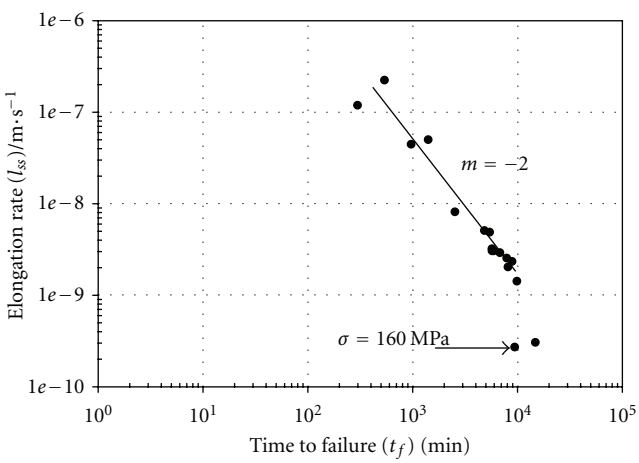

Figure 7: The relations between the logarithms of time to failure (t_f) and steady-state elongation rate (l_{ss}) for A5052-H3 in 0.5 M sodium chloride solution, where m is the slope of the straight line.

an additional local stress in the vicinity of crack tip (σ_{app}) is generated in addition to a local stress caused by applied stress (σ_{app}), where a net local stress (σ_{tip}) = $\sigma_{app} + \sigma_{add}$. When σ_{tip} reaches a critical film fracture stress (σ_{cri}), film fracture occurs. Such a film rupture-formation event is repeated inducing crack propagation until t_{ss} and as a result the steady state elongation rate can be obtained.

5. Conclusions

The following conclusions can be drawn from this work.

(i) The applied stress dependences of the three parameters (t_f, l_{ss}, and t_{ss}/t_f) obtained from the corrosion elongation curve showed that these relationships were divided into three regions, the stress-dominated region, the SCC- or HE-dominated region, and the corrosion-dominated region.

(ii) Aluminum alloy 5052-H3 showed identical behavior in both orientations at all applied stress range.

(iii) The fracture mode for aluminum alloy 5052-H3 was transgranular in both orientations.

(iv) The relationships between $\log t_f$ and $\log l_{ss}$ for the aluminum alloy used became a good straight line. The slope of the line was -2.

References

[1] M. O. Speidel, "Stress corrosion cracking of aluminum alloys," *Metallurgical Transactions A*, vol. 6, no. 4, pp. 631–651, 1975.

[2] M. R. Bayoumi, "The mechanics and mechanisms of fracture in stress corrosion cracking of aluminium alloys," *Engineering Fracture Mechanics*, vol. 54, no. 6, pp. 879–889, 1996.

[3] R. J. Gest and A. R. Troiano, "Stress corrosion and hydrogen embrittlement in an aluminum alloy," *Corrosion*, vol. 30, no. 8, pp. 274–279, 1974.

[4] J. R. Pickens, J. R. Gordon, and J. A. S. Green, "Effect of loading mode on the stress-corrosion cracking of aluminum alloy 5083," *Metallurgical transactions. A*, vol. 14, no. 5, pp. 925–930, 1983.

[5] J. G. Rinker, M. Marek, and T. H. Sanders, "Microstructure, toughness and stress corrosion cracking behavior of aluminum alloy 2020," *Materials Science and Engineering*, vol. 64, no. 2, pp. 203–221, 1984.

[6] W. Y. CHU, Y. B. WANG, and C. M. HSIAO, "Research of hydrogen induced cracking and stress corrosion cracking in an aluminum alloy," *Corrosion*, vol. 38, no. 11, pp. 561–570, 1982.

[7] K. Sieradzki and R. C. Newman, "Stress-corrosion cracking," *Journal of Physics and Chemistry of Solids*, vol. 48, no. 11, pp. 1101–1113, 1987.

[8] S. Suresh, A. K. Vasudevan, and P. E. Bretz, "Mechanisms of slow fatigue crack growth in high strength aluminum alloys: role of microstructure and environment," *Metallurgical Transactions. A*, vol. 15, no. 2, pp. 369–379, 1984.

[9] A. K. Vasudevan and S. Suresh, "Influence of corrosion deposits on near-threshold fatigue crack growth behavior in 2xxx and 7xxx series aluminum alloys," *Metallurgical Transactions. A*, vol. 13, no. 12, pp. 2271–2280, 1982.

[10] R. Nishimura and K. Kudo, "Stress corrosion cracking of AlSl 304 and AlSl 316 austenitic stainless steels in HCl and H_2SO_4 solutions—prediction of time-to-failure and criterion

for assessment of SCC susceptibility," *Corrosion*, vol. 45, no. 4, pp. 308–316, 1989.

[11] R. Nishimura, "The effect of chloride ions on stress corrosion cracking of type 304 and type 316 austenitic stainless steels in sulfuric acid solution," *Corrosion Science*, vol. 34, no. 11, pp. 1859–1868, 1993.

[12] R. Nishimura, "The effect of potential on stress corrosion cracking of type 316 and type 310 austenitic stainless steels," *Corrosion Science*, vol. 34, no. 9, pp. 1463–1473, 1993.

[13] O. M. Alyousif and R. Nishimura, "The effect of test temperature on SCC behavior of austenitic stainless steels in boiling saturated magnesium chloride solution," *Corrosion Science*, vol. 48, no. 12, pp. 4283–4293, 2006.

[14] O. M. Alyousif and R. Nishimura, "The stress corrosion cracking behavior of austenitic stainless steels in boiling magnesium chloride solutions," *Corrosion Science*, vol. 49, no. 7, pp. 3040–3051, 2007.

[15] O. M. Alyousif and R. Nishimura, "Stress corrosion cracking and hydrogen embrittlement of sensitized austenitic stainless steels in boiling saturated magnesium chloride solutions," *Corrosion Science*, vol. 50, no. 8, pp. 2353–2359, 2008.

[16] O. M. Alyousif and R. Nishimura, "On the stress corrosion cracking and hydrogen embrittlement of sensitized austenitic stainless steels in boiling saturated magnesium chloride solutions: effect of applied stress," *Corrosion Science*, vol. 50, no. 10, pp. 2919–2926, 2008.

[17] R. Nishimura, J. Shirono, and A. Jonokuchi, "Hydrogen-induced cracking of pure titanium in sulphuric acid and hydrochloric acid solutions using constant load method," *Corrosion Science*, vol. 50, no. 9, pp. 2691–2697, 2008.

[18] R. H. Jones, Ed., *Stress-Corrosion Cracking*, ASM International, Materials Park, Ohio, USA, 1992.